10512 *Macromolecules* **2010**, *43*, 10512–10520
DOI: 10.1021/ma102273b

Macromolecules
ARTICLE

# High-Pressure-Induced Microstructural Evolution and Enhancement of Thermal Properties of Nylon-6

**Junchun Yu, Bounphanh Tonpheng, and Ove Andersson***

*Department of Physics, Umea University, 901 87 Umea, Sweden*

*Received October 3, 2010; Revised Manuscript Received November 12, 2010*

ABSTRACT: The transition behavior and thermal properties of nylon-6 at elevated pressure, $p$, have been established by in-situ thermal conductivity, $\kappa$, and heat capacity measurements. The glass transition temperature, $T_g$, of virgin nylon-6 is described well by the empirical equation $T_g(p) = 319.60(1 + 1.90\,p)^{0.24}$ ($p$ in GPa and $T_g$ in K). Moreover, isobaric heating in the 1−1.2 GPa range causes a cold-crystallization transition near 500 K. As a result, $\kappa$ increased ∼15% whereas the heat capacity per unit volume decreased ∼7% slowly with time during 4 h annealing at ∼530 K. The transformation is associated with a significantly increased crystallinity, from ∼35% to 55−60%, and a pressure-induced preferred orientation and increased size for the lamellae of monoclinic α crystalline structure. This state has 8−10 K higher melting temperature and better formic acid resistance than that of virgin nylon-6. However, the results show no indication of cross-linking, as reported for similarly treated nylon-1010 and nylon-11, but instead chain scissoring.

## Introduction

Polyamides are a family of synthetic polymers in which units are linked together by amide groups. The most well-known member in this family is nylon, which is the generic name for linear polymers that consist of methylene sequences in between amide groups. Various nylons are referred to by the number of carbon atoms in the constitutional repeating unit, such as nylon-6 with six carbons in the repeat unit: $[CO-(CH_2)_5-NH]_n$. Nylon-6, which is also called polycaprolactam or polyamide-6, is an important engineering thermoplastic and a matrix for composite materials once it has been synthesized. This is mainly due to its high-strength semicrystalline structure that has excellent temperature stability and chemical resistance, which are among the best in the polymer family.[1] Resistance to heat, oil, wear, and abrasion has made nylon an alternative candidate material in applications such as gears, bearings, etc.[1]

Nylon-6 can exist in at least two crystalline modifications: a stable monoclinic α structure and a monoclinic or pseudohexagonal $\gamma$ crystal structure.[1] Slow cooling from the melt yields mainly the former whereas rapid cooling and crystallization at lower temperatures yields increasing amounts of the $\gamma$ phase, and $\gamma$ becomes the dominant phase when crystallization occurs at ∼130 °C and below.[2] The phases may coexist, but the $\gamma$ phase has been found less stable and can be converted to the α form, e.g., by annealing slightly below the melting temperature (493 K) and/or under stress.[1] The remaining amorphous part is in a glassy state at room temperature, but the segmental mobility increases on heating via a weak glass transition. The glass transition temperature $T_g$, which is in the range 320−330 K for dried nylon-6, depends on the thermal treatment and the water content, which has a plasticizing effect in nylon.[1] The glass transition is relatively featureless and therefore difficult to probe, which is an effect possibly caused by the crystalline regions that can restrain the enhanced molecular motions in amorphous regions.[3] The difficulty increases even further under high-pressure conditions, which hamper experimental studies and may also suppress glass transition characteristics such as the change in the thermal expansivity.

There are relatively few experimental studies of nylon-6 under high pressure, and those of a particular interest here are briefly summarized. The glass transition of nylon-6 has been studied by volume measurements at pressures below ∼0.2 GPa.[1] However, $T_g$ was difficult to establish due to only a weak and gradual change in the expansion coefficient, and no equation for the pressure dependence of $T_g$ was given. More recently, Utracki[4] also found it difficult to detect $T_g$ in data for the equation of state of nylon-6, but these results indicated an increase of $T_g$ by 107 K GPa$^{-1}$. It seems that no other study has concerned, or has been able to detect, the $T_g$ variation under high-pressure conditions. Moreover, despite the importance of the thermal conductivity and heat capacity, and their changes with pressure for knowledge in e.g. polymer processing,[5] there seems to be only one previous high-pressure study. Andersson[6] has determined the relative increase of the thermal conductivity of various nylons for pressures up to 2.5 GPa at 300 K. Further, in a series of studies, Gogolewski and Pennings[7−10] have investigated the structural changes in nylon-6 caused by annealing under high-pressure high-temperature (HP&HT) conditions or melting under high pressures below 0.8 GPa. They reported increases of the melting peak temperature and melting enthalpy at atmospheric pressure after such treatments. Moreover, Gogolewski and Pennings[7−10] surmised that the HP&HT treatment caused CO−NH bonds to break and proposed a chain extension mechanism in the crystalline parts of nylon-6, which resulted in larger lamellae sizes and increased crystallinity. This is an interesting effect of pressure noticed for many semicrystalline polymers, e.g., polyethylene[11] and more recently poly($n$-octadecyl methacrylate).[12]

Several synthetic polymers for commercial use are occasionally (e.g., polyethylene) or commonly (e.g., polyisoprene) cross-linked, which is an important method to impart desirable mechanical properties and improved thermal stability. Cross-linkable polymers exhibit improved stiffness and chemical resistance in the cross-linked state fulfilling higher engineering demands than corresponding virgin polymers. Charlesby[13] and Dadbin et al.[14] have shown that it is possible to cross-link "nylon"

*Corresponding author. E-mail: ove.andersson@physics.umu.se.

 Published on Web 11/24/2010 

(nylon-6,6) and nylon-6, respectively, by electron beam radiation. The modified nylon-6 showed enhanced thermal stability, and increased tensile strength and yield stress, but decreased elongation at break.[14] There have also been a number of attempts to cross-link polymers by HP&HT treatments. A few of those concern nylon; e.g., Yang et al.[15,16] studied nylon-1010 treated at 523 K for pressures in the range 0.5−2.5 GPa. They concluded that nylon-1010 became cross-linked during treatment at 1.0 and 1.2 GPa, which was inferred from the absence of melting peaks in subsequent differential scanning calorimetry measurements at atmospheric pressure. Moreover, Gogolewski and Pennings[17] found that nylon-11 could be cross-linked by cooling from the melt or annealing at 593 K or higher at 1.0 GPa. It has also been shown that network formers such as polyisoprene[18] and polybutadiene[19] can be cross-linked into elastomeric states purely by HP&HT treatment, i.e., without the use of vulcanization chemicals. In this work, we have investigated if nylon-6 becomes cross-linked by similar HP&HT treatments.

To the best of our knowledge, this is the first measurements of thermal conductivity, $\kappa$, and heat capacity per unit volume, $\rho c_p$, of nylon-6 in a wide temperature range (100−530 K) under high-pressure conditions. In addition to the magnitudes of $\kappa$ and $\rho c_p$, these data show the glass transition in nylon-6 and, thus, the pressure-induced changes of $T_g$. Moreover, the recovered HP&HT treated samples have been subjected to comprehensive analyses to determine the structural changes. This have enabled us to establish (i) the HP&HT transition behavior and the associated structural changes as well as their effect on $\kappa$ and $\rho c_p$ and (ii) the absence of cross-links in nylon-6 after treatments in 1−1.2 GPa range for temperatures up to 530 K.

## Experimental Section

**Materials and Sample Preparation.** Nylon-6 pellets with a stated viscosity average molecular weight of 10 000 were purchased from Scientific Polymer Products Inc. (The measured viscosity average molecular weight, see below, was 21 000.) The pellets were melted and cast into plates, 5 mm thick and 37 mm in diameter, under dry argon gas. Subsequently, the nylon-6 plates were degassed at 80 °C for 24 h in a vacuum oven before assembling the plates in a sample cell. A sample of nylon-6 was also synthesized using a standard procedure by polymerization of $\varepsilon$-caprolactam, using 6-aminocaproic acid as initiator (see Supporting Information).[20] The measured viscosity average molecular weight was 28 000. The synthesized nylon-6 was cast into plates using the same procedure as for the purchased nylon-6. Unless otherwise stated, the results presented here refer to the purchased nylon-6.

**Thermal Conductivity and Heat Capacity Measurements and High-Pressure Experimental Setup.** The transient hot-wire method, which has been described in more detail earlier,[21] was used to measure simultaneously both $\kappa$ and $\rho c_p$. Briefly, two sample plates were loaded into a custom-made Teflon cell with a hot-wire probe placed in between (Figure 1c). In order to best use the limited space available in the cell as well as to minimize the pressure gradient, the wire was placed in the shape of a circular ring of constant radius. The hot wire was a Ni wire, ~40 mm in length and 0.1 mm in diameter (Figure 1b), which was soldered to lead out wires of copper. The temperature of the sample was measured by a chromel−alumel thermocouple placed in between the sample plates. The thermocouple had previously been calibrated to within ±0.2 K of a commercially calibrated diode sensor, which has an accuracy of 10 mK. Another thermocouple, placed in the Teflon, was used for differential thermal analysis. The Teflon cell was assembled under dry argon gas to avoid reactions with oxygen and decomposition at high temperatures. The Teflon cell was transferred into a piston−cylinder apparatus, which could be heated to ~540 K by an external heater or cooled to low temperatures

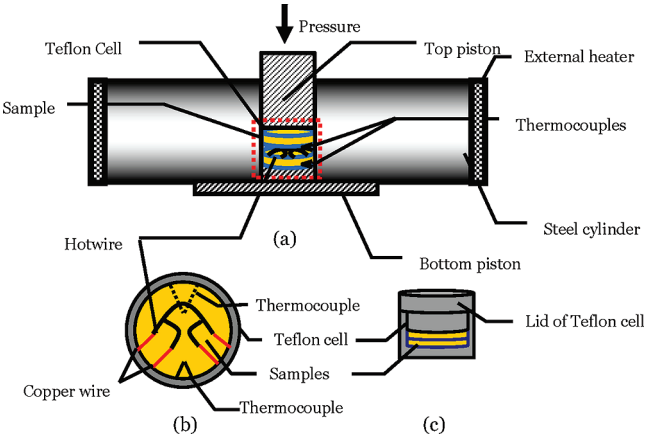


**Figure 1.** Schematic plot of the high-pressure setup: (a) cross-sectional plot of the Teflon cell mounted in the high-pressure cylinder; (b) top view of the Teflon cell with a hot-wire; (c) side view of the Teflon cell; its position in (a) is shown by the dashed square.

(~100 K) using liquid nitrogen. The apparatus has a pressure transmitting top piston and a support bottom piston with electrical feedthroughs (Figure 1a). The electrical resistance heater was controlled using a proportional−integral−derivative (PID) controller control system, which kept the temperature constant to within ±0.5 K under quasi-isothermal experiments. The pressure was generated by a hydraulic press and calculated from load/area with an empirical correction for friction, which had been established using the pressure dependence of a Manganin wire. The maximum pressure inaccuracy was estimated as ±40 MPa at 1 GPa, and the pressure gradient in the probed sample volume, which is within a few millimeters from the hot-wire, is significantly smaller. During the isobaric runs, the pressure was kept to within ±1 MPa using another PID controller.

To determine $\kappa$ and $\rho c_p$, the electronics triggered a 1.4 s long electric pulse of almost constant power, and the hot-wire's resistance was measured as a function of time. The temperature rise of the wire was calculated by using its electrical resistance−temperature relation; i.e., the wire acted as both heater and sensor for the temperature rise. The analytical solution for the temperature rise of the wire was fitted to 29 data points, and $\kappa$ and $\rho c_p$ were thus determined. The inaccuracies were estimated as ±2% in $\kappa$ and ±5% in $\rho c_p$.

**Differential Scanning Calorimetry (DSC).** A Pyris Diamond DSC equipped with intracooler was used for DSC measurements. All the samples used for the DSC measurement were pumped 24 h in a vacuum oven and encapsulated under a nitrogen atmosphere at room temperature to remove water and oxygen. The samples were heated from 20 to 250 °C at scan rate of 10 °C/min and held at 250 °C for 5 min to ensure that the samples were melted before cooling. (However, as discussed further in the Discussion section, small crystallites may still have remained and affected the crystallization behavior on cooling.) Subsequently, the samples were cooled to 20 °C using the same scan rate. The degree of crystallinity $C_{DSC}$ (mass fraction) was calculated from heat of fusion using the total enthalpy method, which yields[22]

$$C_{DSC} = \Delta H / H_{100\%} \times 100\% \quad (1)$$

where $\Delta H$ is the melting enthalpy (J g$^{-1}$) of nylon-6 and $H_{100\%}$ is the extrapolated value for the melting enthalpy of 100% α crystalline nylon-6. Because of the polymorphic behavior of nylon-6, several values of $H_{100\%}$ have been reported in the literature.[23−25] Illers et al.[24] reported a $\Delta H$ of 241 J g$^{-1}$ for the α crystalline form nylon-6, and this value was used here for the calculations of $C_{DSC}$.

**Wide-Angle X-ray Diffraction (WAXD).** WAXD was carried out using a Siemens/Bruker D5000 diffractometer with Cu Kα

radiation at an acceleration voltage of 40 kV and a tube current of 30 mA. The samples were scanned twice from 5° to 50° ($2\theta$) at scanning rate of 4°/min. The first scan was done on the as recovered sample after the HP&HT treatment and the second after the sample had been manually chopped into small grains. The former WAXD spectra were used to determine preferred pressure-induced crystalline orientation, and the latter were used to determine the degree of crystallinity (mass fraction), $C_{WAXD}$, and crystallite size and perfection (CSP). $C_{WAXD}$ was obtained from[1]

$$C_{WAXD} = A_c/(A_c + A_a) \times 100\% \quad (2)$$

$A_c$ and $A_a$ are the integral area of the crystalline and amorphous peak intensities, respectively, which were obtained through fits by Peakfit software.

CSP were determined by the Scherrer equation 1

$$CSP = k\lambda/(\beta \cos \theta) \quad (3)$$

where $\beta$ is the width of the crystalline peak at $2\theta$, $\lambda$ is the X-ray wavelength, and $k$ is a constant equal to 0.9 when $\beta$ is the full width at half-maximum.

**Density Measurements.** The nylon-6 samples were weighted, and the volumes of samples were obtained by quickly immersing these into water at 20 °C. Nylon-6 absorbs water with time but only 1 wt % in 15 min.[26] Thus, the quick procedure of less than 30 s prevented influence by water absorption, which was also verified by ensuring that the weight increase of the sample after the density measurements was negligible. The degree of crystallinity (mass fraction), $C_\rho$, was determined from the equation[27]

$$C_\rho = \left(\frac{1}{\rho_\alpha} - \frac{1}{\rho}\right) / \left(\frac{1}{\rho_\alpha} - \frac{1}{\rho_c}\right) \times 100\% \quad (4)$$

where $\rho$ is the measured density of nylon-6, $\rho_\alpha$ is the density of the amorphous phase (1.098 g cm$^{-3}$),[27] and $\rho_c$ is the density of crystalline nylon-6 (1.220 g cm$^{-3}$).[28,29]

**Viscosity-Average Molecular Weight, $M_w$, Measurement.** Nylon-6 85% formic acid (puriss, 98.0−100%, Sigma-Aldrich) solutions were prepared with solute up to 0.5 g/100 mL for falling-ball viscosity measurements (Thermo Scientific HAAKE falling ball viscometer type B with water bath, Grant Instruments Ltd.). The viscosity-average $M_w$ of nylon-6 was calculated from the Mark−Houwink equation:[30]

$$[\eta] = KM_w{}^a \quad (5)$$

where $[\eta]$ is the intrinsic viscosity, $M_w$ is the viscosity-average molecular weight, and $a$ and $K$ are constants that depend on the particular polymer−solvent system and the temperature.[31] In 85% formic acid at 25 °C, $a = 0.82$ and $K = 2.26 \times 10^{-4}$ dL g$^{-1}$.[31] The intrinsic viscosity is equal to the reduced viscosity, $\eta_{reduced}$, extrapolated to zero solute concentration, and $\eta_{reduced} = (\eta - \eta_0)/(c\eta_0)$, where $\eta$ is the dynamic viscosity of the solution, $\eta_0$ is the dynamic viscosity of the solvent, and $c$ is the solute concentration (g dL$^{-1}$).[1] The dynamic viscosities of the solution and the solvent were obtained from the falling-ball viscosity measurements.

**Formic Acid Treatment.** Nylon-6 samples that had been subjected to HP&HT conditions were placed in formic acid−water solutions of various concentrations to investigate dissolution and gel formation. Virgin nylon-6 dissolves easily in 85% formic acid whereas cross-linked nylon-6 produces a gel, which can be extracted to determine the cross-link density.[32,33] Four different concentrations (50%, 65.7%, 73.3%, 82.3%) of formic acid (puriss, 98.0−100%, Sigma-Aldrich) were prepared by dilution with deionized water for studies at room temperature.

**High-Pressure High-Temperature (HP&HT) Treatment.** As described in the paper, we observe a transition near 500 K at both 1 and 1.2 GPa, which caused significant and irreversible changes of the nylon-6 properties. To differentiate between this state and the initial, or virgin state, we refer to the former, which was obtained by annealing for 4 h at 530 K and 1 or 1.2 GPa, as 1.0 and 1.2 (HP&HT) treated samples.

**High-Temperature (HT) Annealing Experiment.** A sample of virgin nylon-6 was annealed in argon atmosphere at 493 K for 7 days in order to reach a similar degree of crystallinity as the samples treated under HP&HT conditions. This sample (HT annealed sample) was studied by $M_w$, DSC, and WAXD measurements and by treatment in formic acid to assess the influence of crystallinity and crystal size on the thermal stability and dissolution properties and to compare the lamellae growth at HT and 1 atm with that of the HP&HT samples.

## Results

**Hot-Wire Measurement of $\kappa$ and $\rho c_p$.** The temperature scans of nylon-6 were performed under isobaric conditions for temperatures in the range 100−500 K at 9 pressures up to 1.2 GPa. In general, the sample was heated to above the glass transition of nylon-6 before the measurements commenced to avoid significant thermal history effects caused by pressurizing or depressurizing below the glass transition. Results of $\kappa$ and $\rho c_p$ at isobaric conditions are shown in Figure 2.

As shown in Figure 2, $\kappa$ is almost constant or weakly increasing with temperature. Moreover, for the virgin samples, i.e., samples that had not been subjected to HP&HT conditions (see Experimental Section for details) there is a distinct change in $d\kappa/dT$ above room temperature. For example, $d\kappa/dT$ changes from positive to negative near 410 K at 1 GPa, which is a typical behavior at glass transitions in polymers as well as many other materials.[34] This result is also confirmed by the behavior of the simultaneously measured data for $\rho c_p$. These show a (stretched weak) sigmoidal increase, which is characteristic of a glass transition (Figure 2a,b). This feature was, however, occasionally less distinct than that in $\kappa$, which is due to the better precision in $\kappa$ and that the temperature derivative of $\kappa$ changes sign at $T_g$. For that reason, we have used the values of $\kappa(T)$ to establish $T_g(p)$ of nylon-6.

The results for $T_g(p)$ (Figure 3), extracted from the results for $\kappa(T)$, show the typically observed pressure-induced increase, which levels off at high pressures. For comparison, we have also plotted values of the melting temperature taken from Gogolewski and Pennings.[9] The values for $T_g(p)$ are described well by the empirical equation[35]

$$T_g(p) = T_0\left(1 + \frac{b}{a}p\right)^{1/b} \quad (6)$$

where $a$, $b$, and $T_0$ are fitting parameters and $p$ is the pressure in GPa. The fit yielded $T_0 = 319.60$ K, $a = 2.19$ GPa, and $b = 4.17$. For comparison, DSC measurements at 1 bar on a sample which had been quenched from the melt yielded $T_g = 311.5$ K (onset temperature[3]).

On heating at 1 GPa, a transition occurred at 494 K, which caused the measurements to fail abruptly and the transformation could therefore not be monitored in the data. The sample was heated to 530 K and held for 4 h without measurements (HP&HT treatment) and thereafter cooled to room temperature and recovered for further measurements using a new hot-wire probe. These showed that the HP&HT treatment had increased $\kappa$ about 15% while $\rho c_p$ had decreased 7% at room temperature. Moreover, heating at 1 GPa showed that the glass transition features in both $\kappa$ and $\rho c_p$ had vanished. That is, the distinct change in $d\kappa/dT$ could not be observed, and the slope of $\rho c_p$ remained unchanged on heating (Figure 2a,c), which was also the case in subsequent measurements at other isobars.

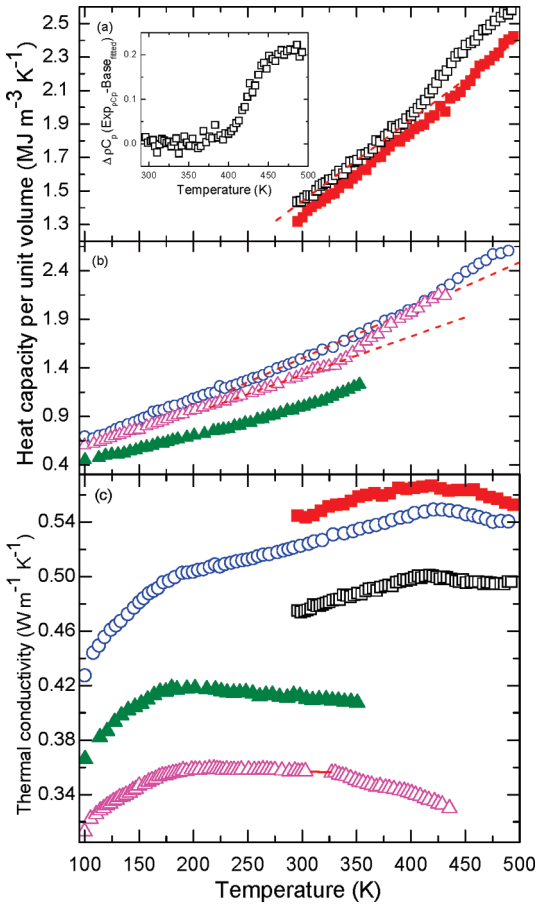


**Figure 2.** (a, b) Heat capacity per unit volume and (c) thermal conductivity of nylon-6 measured on heating. The open symbols are for virgin nylon-6 samples at (△) 0.07, (□) 1.0, and (○) 1.2 GPa, whereas the solid symbols are for 1.0 GPa HP&HT treated nylon-6 samples at (▲) 0.07 and (■) 1.0 GPa. The inset in (a) shows the excess heat capacity per unit volume, $\Delta\rho c_p$, for virgin nylon-6, which was calculated by subtracting a linear function, fitted below 296 K, from the experimental data. The dashed red lines in (a) and (b) represent linear fits of data below the slope change of the curve. The red solid line in (c) shows a range where the measurements were disturbed by a phase transition in Teflon (sample cell), and the data were therefore omitted.

In order to establish the nature of the transformation, it was studied by differential thermal analysis (DTA) during heating at an average rate of 0.45 K/min to 540 K at 1 GPa and then cooled at 0.5 K/min and recovered at 1 atm for WAXD analysis, which showed that the crystallinity had increased from 37% to 42%. The DTA data, however, showed no indication of an exothermic (or endothermic) transition.

In an experiment with a different nylon-6 sample, which had been synthesized by polymerization of ε-caprolactam (see Experimental Section), we did succeed to monitor the transition in data for $\kappa$ at 1 GPa and 530 K (Figure 4a). This sample had slightly higher initial molecular weight than the purchased nylon-6 sample. The results show that $\kappa$ increases about 15% slowly during 6 h, i.e., about the same increase as for purchased nylon-6, and a fit of an exponential function gave a time constant of ~3 h. WAXD analysis showed that the treatment had increased the degree of crystallinity from 39% to 56%.

Figure 4b shows results for $\kappa$ on pressurization at 298 K both before and after the transformation caused by the HP&HT treatment (1.0 GPa). The results of virgin nylon-6 exhibit a pressure-dependent increase up to 0.5 GPa, which is described to within ±0.5% by the equation

$$\kappa_{\text{virgin}} = 0.345 + 0.174p - 0.0727p^2 \qquad (7)$$

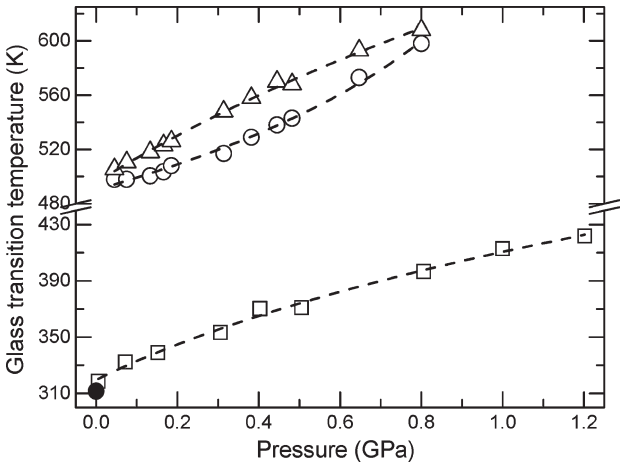


**Figure 3.** Glass transition temperature of virgin nylon-6 plotted against pressure: (□) $T_g$ obtained by the hotwire method; (●) $T_g$ obtained by DSC at atmospheric pressure. The dashed line represents a fit of eq 6. Melting temperature plotted against pressure for virgin nylon-6 from ref 9: (○) onset and (Δ) finish of melting.

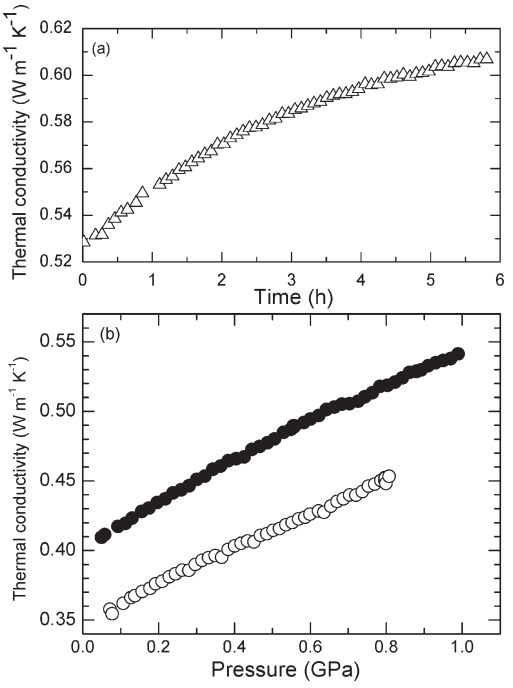


**Figure 4.** (a) Thermal conductivity of a nylon-6 sample made by polymerization of ε-caprolactam (see Experimental Section) plotted against time at 1.0 GPa and 530 K. (The fractional increase of $\kappa$ is about the same as for the similarly treated purchased nylon-6 sample, but the initial value is about 6% higher than for the purchased nylon-6.) (b) Thermal conductivity of (purchased) nylon-6 on pressurization at 298 K before (○) and after (●) 1.0 GPa HP&HT treatment.

where $p$ is the pressure in GPa ($\kappa$ in W m$^{-1}$ K$^{-1}$). The 1.0 GPa treated nylon-6 shows a similar tendency as virgin nylon-6, but with a higher initial $\kappa$, and for pressures up to 0.5 GPa this is described by

$$\kappa_{\text{treated}} = 0.401 + 0.179p - 0.0421p^2 \qquad (8)$$

In another experiment of (virgin) nylon-6 at 1.2 GPa, a similar transition was observed at ca. 492 K when the sample was heated to 530 K. Also in this case the hot-wire probe broke abruptly, and therefore no data were recorded. However, the sample was recovered for analysis of the structural and property changes after a 4 h anneal at 530 K and 1.2 GPa.

**Table 1. Formic Acid Extraction Tests of Nylon-6 Samples after Various Treatments (See Experimental Section for Details)[a]**

| | virgin | HT annealed | 1.0 GPa treated | 1.2 GPa treated |
|---|---|---|---|---|
| 82.3% formic acid | – | D | D | D |
| 73.3% formic acid | – | D | D | P |
| 65.7% formic acid | – | P | P | P |
| 50% formic acid | D | – | – | – |

[a] D: dissolved; P: partly dissolved.

**Investigation of Cross-Link Properties by Formic Acid Extraction.** After HP&HT treatments, the samples were immersed in formic acid to study gel formation, which takes place if a sample is cross-linked.[32,33] Even though the samples exhibited different degree of stability in formic acid, none showed gel formation. As shown in Table 1, both the 1.0 and 1.2 GPa treated samples dissolved in 82.3% formic acid. The 1.0 GPa treated sample also dissolved in 73.3% formic acid, whereas the 1.2 GPa treated sample only partially dissolved. Neither the 1.0 nor the 1.2 GPa treated sample could be completely dissolved in 65.7% formic acid. The HT annealed sample (see Experimental Section) could be dissolved in 73.3% formic acid but only partially dissolved in 65.7% formic acid. As a reference, a virgin sample could be dissolved in 50% formic acid. The residual pieces of the 1.2 GPa treated sample after the 73.3% formic acid extraction (1.2 GPa AE sample) were collected for further investigation.

**Degree of Crystallinity, Structural Properties, and Transition Behavior by WAXD, DSC, and Density Measurements.** The monoclinic α structure of nylon-6 has two principal diffraction peaks at 19.9° (α1) and 23.75° (α2), which are due to the (200) and (002) + (202) planes, respectively.[8] (200) are planes along the molecular chains but cutting through hydrogen-bonded sheets. The (002) planes lie parallel to the hydrogen-bonded sheets, where (202) is the diagonal plane.[1] The γ structure has a principal diffraction peak at 22°.[1] The amorphous part of nylon-6 gives a broad diffuse halo with an intensity maximum at ca. 22°.[1]

As shown in Figure 5, the virgin nylon-6 had the α crystal structure with almost equal intensities for α1 and α2. In the case of the 1.2 GPa HP&HT treated sample plate, which was mounted with the axis of rotation in the same direction as the applied pressure (Figure 5, top left), the intensity of α2 increased significantly compared to α1. However, after chopping the sample into small grains (Figure 5, top right), the original WAXD spectrum was recovered. The spectrum of the HT annealed nylon-6, which was in a granular form, was equal to that for the virgin sample, but with a weaker broad peak associated with the amorphous parts.

As tabulated in Table 2, the HP&HT treated samples (both 1.0 and 1.2 GPa treated) achieved higher density than a cast virgin nylon-6 sample. This also results in a higher degree of crystallinity ($C_\rho$), which was obtained by eq 4. The analysis of the WAXD spectra, using eq 2, gave similar results. The HP&HT treated samples showed higher degree of crystallinity ($C_{WAXD}$) in comparison with the virgin sample. Moreover, the full width at half-maximum of the crystalline peak of the HP&HT treated samples was narrower, which corresponds to larger crystal sizes (eq 3) than for the other samples. The HT annealed sample showed a large increase of crystallinity, compared to the virgin sample, but smallest crystal sizes among all the samples.

DSC was applied to establish the melting temperature ($T_{melt}$), melting on-set temperature ($T_{onset}$), transition enthalpy ($\Delta H$), and crystallization temperature ($T_{cry}$) of the nylon-6 samples. As shown in Figure 6, both virgin and

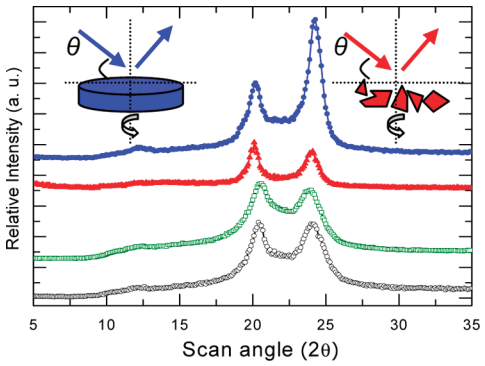


**Figure 5.** WAXD spectra of nylon-6 samples (from bottom to top): 1, virgin nylon-6; 2, HT annealed nylon-6; 3, randomly arranged particles of 1.2 GPa treated nylon-6 (inset at top right); 4, plate-shaped 1.2 GPa treated nylon-6 (scanned as shown by the top-left image with the axis of rotation in the same direction as the applied pressure). Scans are shifted for clarity.

**Table 2. Crystallinity ($C_{WAXD}$ and $C_\rho$), Density, and Crystal Size and Perfection (CSP) of Nylon-6 Samples[a]**

| | | | | CSP | |
|---|---|---|---|---|---|
| sample | $C_{WAXD}$ (%) | density (g/cm$^3$) | $C_\rho$ (%) | α1 (Å) | α2 (Å) |
| virgin | 37 | 1.149 | 44 | 76.8 | 51.4 |
| HT annealed | 65 | | | 33.8 | 49.2 |
| 1.0 GPa treated | 52 | 1.174 | 65 | 84.0 | 75.1 |
| 1.2 GPa treated | 55 | 1.180 | 69 | 96.0 | 85.5 |
| 1.2 GPa treated AE | 48 | | | 93.8 | 75.2 |

[a] The high crystallinity of the HT annealed sample is partly software related as the crystalline peaks were significantly broadened, and as a consequence, a part of the broad amorphous peak was included in the integral area of the crystalline peaks.

HP&HT treated nylon-6 exhibit an endothermic melting peak at ca. 220 °C on heating, followed by an exothermic crystallization dip at ca. 180 °C on cooling, but there is no indication of a glass transition feature. The data from the first and second heating and cooling runs, including heat of fusion based crystallinity ($C_{DSC}$), are listed in Tables 3 and 4.

The HP&HT treated samples showed higher $T_{melt}$, $T_{onset}$ (~11 K), and $\Delta H$, i.e., also $C_{DSC}$, on the first heating than the virgin sample. On the first cooling run, the HP&HT treated samples showed higher $T_{cry}$ (~13 K) compared to the virgin and the HT annealed samples. Moreover, the 1.2 GPa treated AE sample exhibited the highest $T_{melt}$ (~11 K higher than nylon-6), $T_{onset}$ (~17 K higher than nylon-6), and $T_{cry}$ (~16 K higher than nylon-6) among the HP&HT treated samples. In contrast, the HT annealed sample had slightly higher $T_{melt}$ and $\Delta H$, similar $T_{cry}$, but lower $T_{onset}$ compared to virgin nylon-6.

On the second heating run (Table 4), $T_{melt}$, $T_{onset}$, and $\Delta H$ of the HP&HT treated samples decreased compared to first heating. The values for $T_{melt}$ were only ~4 K higher than that of virgin nylon-6, and $\Delta H$ and $T_{onset}$ were similar to those of virgin nylon-6. However, $T_{cry}$ remained almost unchanged, i.e., significantly higher than for virgin nylon-6. The HT annealed sample showed almost the same results as the virgin material. This means that $C_{DSC}$ became essentially the same for all samples after the first heating and cooling runs.

**Molecular Weight ($M_w$) Measurements by Falling-Ball Viscosimetry.** As tabulated in Table 5, the viscosity-average $M_w$ of nylon-6 decreased after the HP&HT treatment with a slight pressure-sensitive tendency. The 1.0 and 1.2 GPa treated samples were reduced to 86% and 76%, respectively, of their original values. The 1.2 GPa AE sample obtained the

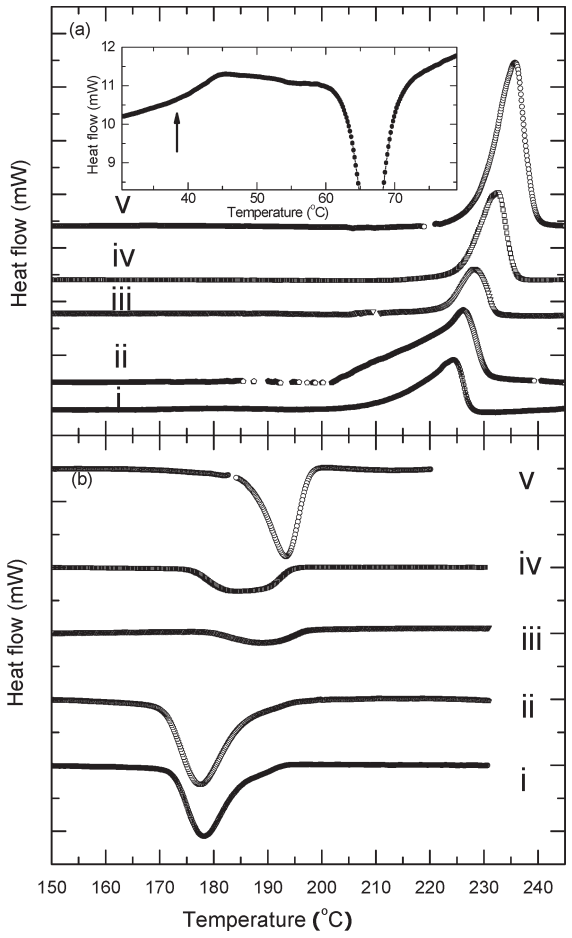


**Figure 6.** DSC traces of nylon-6. (a) First heating run (from bottom to top): i, virgin; ii, HT annealed; iii, 1.0 GPa treated; iv, 1.2 GPa treated; v, 1.2 GPa treated AE. (b) First cooling run: the sequence and label of spectra are the same as in (a). Inset in (a) shows the DSC trace of nylon-6 after the DSC pan had been heated to 250 °C and quenched in liquid nitrogen to obtain a highly amorphous phase. The results show the glass transition (arrow) followed by cold crystallization near 65 °C. Scans are shifted for clarity.

**Table 3. Results of the First DSC Heating and Cooling Runs**

| sample | $\Delta H$ (J/g) | $C_{DSC}$ (%) | $T_{melt}$ (°C) | $T_{onset}$ (°C) | $T_{cry}$ (°C) |
|---|---|---|---|---|---|
| virgin | 56.8 | 24 | 222.9 | 210.9 | 178.2 |
| HT annealed | 80.3 | 33 | 226.3 | 201.5 | 177.3 |
| 1.0 GPa treated | 124.8 | 52 | 230.6 | 222.7 | 191.0 |
| 1.2 GPa treated | 142.4 | 59 | 232.8 | 225.6 | 191.4 |
| 1.2 GPa treated AE | 130.7 | 54 | 234.0 | 228.0 | 194.0 |

**Table 4. Results of the Second DSC Heating and Cooling Runs**[a]

| sample | $\Delta H$ (J/g) | $C_{DSC}$ (%) | $T_{melt}$ (°C) | $T_{onset}$ (°C) | $T_{cry}$ (°C) |
|---|---|---|---|---|---|
| HT annealed | 54.2 | 23 | 225.4 | 213.2 | 177.7 |
| 1.0 GPa treated | 42.6 | 18 | 225.5 | 216.8 | 189.6 |
| 1.2 GPa treated | 52.8 | 22 | 226.6 | 211.7 | 192.0 |
| 1.2 GPa treated AE | 70.7 | 29 | 226.3 | 211.7 | 193.9 |

[a] The results for virgin nylon-6 were identical during first and second heating.

lowest $M_w$ of all samples, almost one-fifth of the original value. For comparison, 7 days of annealing at 493 K decreased the $M_w$ to 90% of the original value.

## Discussion

**Glass Transition of Nylon-6 before and after HP&HT Treatment.** In comparison with many other amorphous polymers, the glass transition temperature $T_g$ of nylon-6 is difficult to probe, especially at high pressures, which is partly explained by the semicrystallinity of nylon-6. A three-phase model of nylon-6 was recently suggested by Chen et al.,[36] comprising crystalline, mobile amorphous, and rigid amorphous fractions. In this model, only a fraction of the amorphous parts become mobile at the glass transition, which would further diminish the changes at $T_g$. This may explain why it is difficult to determine $T_g$ of nylon. However, although the effect of $T_g$ is weak in data for $\kappa$, it is clearly detected.

**Table 5. Molecular Weight (Viscosity Average) and Intrinsic Viscosity of Nylon-6 Obtained from Falling-Ball Viscosity Measurements**

| sample description | $M_w$ | intrinsic viscosity (dL/g) |
|---|---|---|
| virgin | 21 000 | 0.80 |
| HT annealed | 19 000 | 0.73 |
| 1.0 GPa treated | 18 000 | 0.69 |
| 1.2 GPa treated | 16 000 | 0.62 |
| 1.2 GPa treated AE | 4 400 | 0.22 |

In temperature scans of $\kappa$, shown in Figure 2, it is possible to discriminate two ranges above room temperature with about constant, but different, $d\kappa/dT$. The slope changes rather abruptly from positive to negative on heating, e.g., at ca. 430 K at 1.2 GPa. The change is due to the increased thermal expansivity at $T_g$ and the correspondingly stronger decrease of density above $T_g$ than below, which often yields a maximum in $\kappa$ at $T_g$.[34,37] The change in $\kappa(T)$ generally agree well with the change in the slope of the concurrently measured data for $\rho c_p$. Since the density decreases weakly with temperature, the increase in $\rho c_p$ is due to an increase of the heat capacity. Heat capacity data normally show a more distinct sigmoidal increase at $T_g$, but the weak change for nylon-6 is consistent with the weak glass transition features in other properties. The heat capacity step at $T_g$ is apparently small and gradual for nylon-6. The result for the initial slope of $T_g$ obtained from eq 6, $dT_g/dp = 126$ K GPa$^{-1}$, is in fair agreement with the result of Utracki[4] (107 K GPa$^{-1}$). We also note that the pressure-induced increase of the melting temperature is stronger than that of $T_g$ and, therefore, that an extrapolation based on the change of the melting temperature does not provide an accurate estimate of $T_g$ at high pressure.

Since $T_g$ depends on the time scale of the measurements, it is natural that the value of DSC measurements using a heating rate of 10 K min$^{-1}$ is lower than that of the hot-wire measurements with a heating rate of ~150 K min$^{-1}$ (heating pulse of 3.5 K for 1.4 s; see Experimental Section). The former gave $T_g = 311.5$ K, whereas the value of the latter, extrapolated to atmospheric pressure, is $T_g = 319.60$ K, i.e., about 8 K higher, which is the difference typically observed.[35,38]

After HP&HT treatment, all the $T_g$ features vanished, which suggests that most of the configurational contribution that contribute to the heat capacity increase at the glass transition were lost. This implies an amorphous to crystalline structural conversion during the HP&HT treatment and/or a conversion of mobile to rigid amorphous fractions.[36]

**Nature of the HP&HT Transformation.** The transformation, which was detected at ~494 K on heating in the 1−1.2 GPa range, proceeds slowly with time in data for $\kappa$, which showed a time constant of ~3 h at 530 K and 1 GPa for our synthesized sample (Figure 4a). WAXD results show that the structure of the recovered HP&HT treated samples (α structure) does not change but that the crystallinity increases with annealing time above ~500 K in the 1−1.2 GPa range. We can therefore conclude that the transition is a sluggish cold crystallization process. Crystallization becomes energetically more favorable under pressure due to the reduction of

volume. It is kinetically restrained at low temperatures, but the temperature-induced increase of mobility makes it possible at ~500 K for nylon-6. This may be associated with the increased mobility suggested at the subtle Brill transition, which is observed at ~170 °C (443 K) and 1 atm.[39]

The viscosity results of the recovered samples show that the $M_w$ of nylon-6 decreased after the HP&HT treatment; i.e., the treatment caused chain scissoring. Since the $M_w$ of the 1.2 GPa treated AE sample decreased to 21% of the original $M_w$, whereas the corresponding (average) value for the 1.2 GPa treated sample was 76%, we can conclude that this was not a homogeneous process in the sample. Gogolewski[10] reported that amide bonds were transamidated or broken at adjacent lamellae during HP&HT treatment of nylon-6 below 0.8 GPa. This was inferred from infrared spectroscopy and the absorption in the range 3400−3500 $cm^{-1}$ assigned to unbonded N−H groups. We cannot observe a similar change in Raman and Fourier transform infrared spectroscopy (FTIR) spectra measured here (see Supporting Information), but since this has also been suggested for nylon samples at atmospheric pressure and below 300 °C, it is most likely the origin of the scissoring.[40] As the sample with the lowest $M_w$ still have in average only four breaks per chain, it may explain why it escapes detection in Raman and FTIR measurements.

The formic acid extraction tests showed that the nylon-6 had better acid resistance after the HP&HT treatment. A similar tendency, but less pronounced, was also observed for the HT annealed sample. The HP&HT treated samples are characterized by a higher degree of crystallinity (Tables 2 and 3) and a lower $M_w$ than virgin nylon-6 (Table 5). As described quantitatively by the Ostwald−Freundlich equation,[41,42] a crystalline sample is energetically more stable and therefore less soluble than an amorphous counterpart. This is in correspondence with the increase of crystal size during the HP&HT treatment (Table 2). For the HT annealed sample, the crystal size obtained from the WAXD data decreased, which is probably due to many new small lamellae produced during annealing. But the annealing should also have increased the size of other lamellae, which is indicated by the DSC results. For the same reason as the dissolution is dependent on crystal size, the shape of the DSC melting endotherm is determined, at least partly, by the distribution in lamella thickness.[43,44] The melting peak of the HT annealed sample shows a broad peak with a low onset temperature due to many new thin lamella, but also an increase of the peak melting temperature, due to an increase of lamella thickness for some crystals. The most significant increase of $T_{melt}$ is for the 1.2 GPa treated AE sample, which also achieved the best formic acid resistance. We can conclude that the formic acid resistance improves for the HP&HT treated samples and that this is consistent with the observed increase of the lamella size.

Previous results[15,16] have suggested that nylon-1010 becomes cross-linked by heating to 523 K at pressures in the range 1.0−1.2 GPa. The results shown here indicate that a similar HP&HT treatment for nylon-6 does not induce cross-links although the sample was annealed for 4 h at about 500 K to allow for a possible sluggish cross-link process. In particular, the lack of gel formation by HP&HT treated nylon-6 in formic acid provides negative evidence. Furthermore, WAXD data show improved crystallinity after the HP&HT treatment, whereas cross-linking typically decreases the crystallinity.

**Crystal Structure, Degree of Crystallinity, and Orientation of Nylon-6 Lamellae.** It is perspicuous that the HP&HT treatment improves the crystal structure and, as discussed below, induces a preferred crystal orientation. During the transformation, polymer chains pertaining to the amorphous parts folds into the α structure, and a significant amorphous fraction converts to crystalline, which is shown by the WAXD data. Gogolewski and Pennings[9] have previously studied HP&HT treated nylon-6 and also found an increased crystallinity and increased lamellae sizes at pressures below 0.8 GPa. Moreover, they observed similar, but less pronounced, changes in the α1 and α2 peak heights of the WAXD spectra but provided no explanation for these changes.

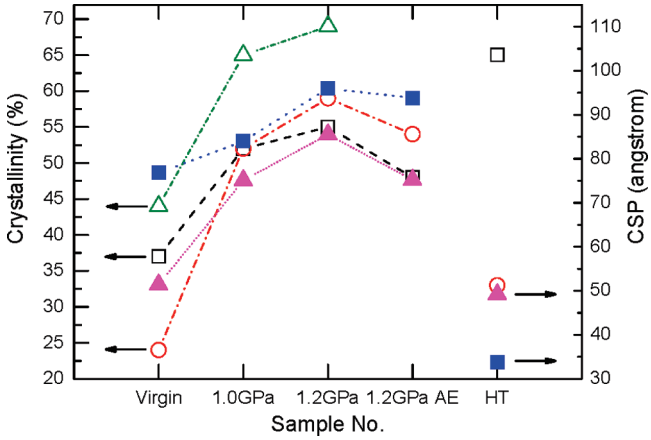


**Figure 7.** Degree of crystallinity of nylon-6 samples obtained from (△) $C_\rho$, (□) $C_{WAXD}$, and (○) $C_{DSC}$. Crystal size and perfection CSP of nylon-6 samples obtained from WAXD measurement: (■) and (▲) represent the CSP calculated from the α1 and α2 peaks, respectively. The lines are plotted to guide the eye.

The general tendency of an increased degree of crystallinity with increasing pressure for the HP&HT treatment is in good agreement between the different analyses based on WAXD, density, and DSC data (Figure 7). These results taken together show that the crystallinity of nylon-6 increases about 25%, from ~35% to 60% (average values), by the 1.2 GPa treatment. The increase of crystallinity for the HP&HT treated samples may occur both in the fully amorphous parts, i.e., growth of new lamellae, and at the boundaries of lamellae, which increases the lamellae sizes. The increased melting temperature, sharp melting endotherm, and improved formic acid resistance favor the latter, or at least that the process results in enlarged lamella sizes with a narrow distribution. This deduction is in good agreement with the CSP results shown in Figure 7. The CSP data show that the crystal sizes increase systematically with increasing pressure of the HP&HT treatment. Moreover, the calculated crystal sizes are larger than that of the HT annealed sample. Apparently, the HP&HT lamella growth process is significantly different from that occurring at atmospheric pressure HT annealing. The latter gives a wide distribution of lamella sizes with many new thin lamellae, which is shown by the broad melting endotherm with a low onset temperature. The growth of many new small sized lamellae explains the decrease of the crystal size obtained in the CSP analysis.

As shown by the WAXD spectra (Figure 5), the intensities of α2 and α1 peaks were about the same for virgin and HT annealed samples, whereas α2 increased to 3 times the size of α1 after the 1.2 GPa treatment. But after the HP&HT treated sample had been chopped to ensure random orientation of the crystals, the α2 and α1 peaks again exhibited similar intensities. This shows that the lamellar growth must have a preferred direction during the HP&HT treatment and that the crystal planes causing the α2 peak become parallel to the sample plate (see inset of Figure 5), which is not the case for

the HT sample. A similar effect has been observed for nylon-6 subjected to shear forces, e.g., in die compression with uniaxial flow.[45] This treatment caused the chain axis to align in the direction of flow, and the hydrogen-bonded sheets, i.e., the (002) planes, slip and become oriented with the sheets perpendicular to the compression direction, which increased the α2 peak while the α1 peak diminished when the sample was scanned in the same manner as done here. Thus, we find that HP&HT treatment in a piston−cylinder device causes the hydrogen-bonded sheets and, therefore also, the polymer chains to become preferably oriented parallel with the sample plate surface, i.e., perpendicular to the applied load. Since the nylon-6 lamellae consist of hydrogen-bonded sheets of folded polymer chains stacked upon one another, it follows that the treatment promotes folding within the plane perpendicular to the applied load. But due to the absence of (uniaxial) flow during the treatment here, the chains of different lamellae would be randomly oriented within this plan. Moreover, since the α1 peak remained unaffected, it presumably means that the existing lamellae did not reorient by the treatment.

**Thermal Stability of the HP&HT Produced State.** The DSC results show that the 1.2 GPa treated AE sample had the highest $T_{melt}$ and the sharpest melting peak. As discussed above, this behavior is likely due to larger lamellae with a narrow distribution of sizes, which result in improved thermal stability as well as better acid resistance. After melting, these differences between the HP&HT treated and virgin samples essentially vanished, but a difference in crystallization temperature still remained.

At the second heating and cooling runs, $T_{melt}$ of the HP&HT treated samples had decreased to about the same as virgin nylon-6, whereas $T_{cry}$ was more than 10 K higher. When a polymer sample is cooled, the crystallization process is initially controlled by their nucleation rate, which typically decreases with increasing temperature well above $T_g$. However, fragments of micro- or submicroscopic crystalline structures may persist in a melt for long time, referred to as crystalline memory, and on cooling these serve as nuclei, thereby promoting the crystallization process. Since we have already concluded that the HP&HT treatment produced lamellae with improved stability, it is not surprising that crystalline domains persisted in the melt and caused a higher $T_{cry}$ on cooling.[37]

**Effect of the Pressure-Induced Structural Changes on $\kappa$ and $\rho c_p$.** As generally observed for polymers, $\kappa$ of nylon-6 increases on isothermal pressurization. This is a reversible change where the lattice elastically deforms and the volume decreases while the phonon frequency and velocity increase. At room temperature, the volume of nylon-6 decreases 3.6% up to 0.19 GPa, which corresponds to a decrease of the intermolecular distance of ∼1.3%.[4] Simultaneously, $\kappa$ increases 9%, which yields a density dependence of $\kappa$ of $g = 2.5$, where $g = (\partial \ln \kappa)/(\partial \ln \rho)$. This is in the range of about 2−6 observed previously for semicrystalline polymers.[46] Moreover, the 29% increase of $\kappa$ up to 1.0 GPa (eq 7) is in fair agreement with the previously reported 40% increase.[6]

During the HP&HT treatment, the structure changes irreversibly when the lamella size increases and new lamellae grow while the average chain length decreases about 15%. The latter is slightly detrimental for the heat transport whereas the more ordered structure with a preferred lamella orientation promotes the heat transport. (If $\kappa$ of nylon-6 varies with $M_w$ in the same manner as for molten linear polyethylene,[47] we deduce that the decrease of $M_w$ established here would cause a less than 3% decrease of $\kappa$.) We can conclude that $\kappa$ of nylon-6 increases ∼15% as a result of a crystallinity increase from 35% to 55% and a preferred crystal orientation, which was caused by the HP&HT treatment at 1 GPa. This seems as a rather moderate increase of $\kappa$ considering the 20% increase of crystallinity. Apparently, the large thermal resistivity due to amorphous domains in between the lamellae limits the decrease of resistivity, in a similar manner as a large resistance does in a series coupling of resistances.

The decrease of $\rho c_p$ caused by the HP&HT transformation is due to a decrease of $c_p$, which surmounts the simultaneous increase of $\rho$. The amorphous to crystalline transformation accounts for the decrease as a crystalline lamella has lower $c_p$ than an amorphous counterpart above $T_g$. The difference diminishes below $T_g$ due to the loss of the configurational heat capacity for the (mobile) amorphous fractions. The remaining difference must be due to the change in the vibrational part of the heat capacity upon crystallization, which may also include fractions that do not crystallize because of interaction between lamellae and the amorphous interlamella regions. As a result, $\rho c_p$ decreases ∼7% at room temperature because of the HP&HT treatment at 1.0 GPa.

## Conclusions

The pressure-induced change of the glass transition temperature of nylon-6 has been established by simultaneous measurements of thermal conductivity and heat capacity. The change was ascertained by observations of a maximum in the thermal conductivity and a (weak) sigmoidal heat capacity increase, which are typical glass transition features.

A transformation observed at ∼494 K on heating at 1.2 GPa (and 1 GPa) is due to cold crystallization. After subsequent annealing for 4 h at ∼530 K, the degree of crystallinity of nylon-6 had increased from 35% to as much as 60%, and the glass transition features had vanished. This treatment increases the lamella regions through growth of lamellae in a preferred direction, which likely occurred through chain folding in a plane perpendicular to the applied load. Concurrently, the chain length decreased slightly through chain scissoring. This result is different from previous results for nylon-1010, which has been found to have cross-links after a similar treatment.[15,16]

The new and more ordered state of nylon-6, in which the lamellae are larger and have a preferred orientation, has better thermal stability and formic acid resistance. It also has about 15% higher thermal conductivity than the virgin state. But considering the large increase of the crystallinity, the thermal conductivity enhancement is probably limited by a large thermal resistance in the amorphous interlamella regions. For the purpose of achieving better thermal conductivity it is probably necessary to reduce the interlamella resistance.

**Acknowledgment.** This work was financially supported by Swedish Research Council.

**Supporting Information Available:** FTIR spectra of 1.0 GPa treated and virgin nylon-6; experimental procedure of synthesis of nylon-6. This material is available free of charge via the Internet at http://pubs.acs.org.

## References and Notes

(1) Kohan, M. I. *Nylon Plastics Handbook*; Hanser/Gardner Publications, Inc.: Cincinnati, OH, 1995.
(2) Kyotani, M.; Mitsuhashi, S. *J. Polym. Sci., Part A-2: Polym. Phys.* **1972**, *10*, 1497–1508.
(3) Hatakeyama, T.; Quinn, F. X. *Thermal Analysis: Fundamentals and Applications to Polymer Science*, 2nd ed.; John Wiley & Sons, Inc.: Chichester, 1999.

(4) Utracki, L. A. *J. Polym. Sci., Part B: Polym. Phys.* **2009**, *47*, 299–313.
(5) Kovarskii, A. L. *High-Pressure Chemistry and Physics of Polymers*; CRC Press: Boca Raton, FL, 1994.
(6) Andersson, P. *Makromol. Chem.* **1976**, *177*, 271–277.
(7) Gogolewski, S.; Pennings, A. J. *Polymer* **1975**, *16*, 673–679.
(8) Gogolewski, S.; Pennings, A. J. *Polymer* **1977**, *18*, 647–653.
(9) Gogolewski, S.; Pennings, A. J. *Polymer* **1977**, *18*, 654–659.
(10) Gogolewski, S. *Polymer* **1977**, *18*, 63–68.
(11) Kurtz, S. M. *UHMWPE Biomaterials Handbook: Ultra High Molecular Weight Polyethylene in Total Joint Replacement and Medical Devices*, 2nd ed.; Elsevier: Amsterdam, 2009.
(12) Mierzwa, M.; Floudas, G.; Štepánek, P.; Wegner, G. *Phys. Rev. B* **2000**, *62*, 14012–14019.
(13) Charlesby, A. *Nature* **1953**, *171*, 167–167.
(14) Dadbin, S.; Frounchi, M.; Goudarzi, D. *Polym. Degrad. Stab.* **2005**, *89*, 436–441.
(15) Yang, J.; Dong, W.; Luan, Y.; Liu, J.; Liu, S.; Guo, X.; Zhao, X.; Su, W. *J. Appl. Polym. Sci.* **2002**, *83*, 2522–2527.
(16) Yang, J.; Liu, S.; Guo, X.; Luan, Y.; Su, W.; Liu, J. *Macromol. Chem. Phys.* **2002**, *203*, 1081–1087.
(17) Gogolewski, S.; Pennings, A. J. *Polymer* **1977**, *18*, 660–666.
(18) Tonpheng, B.; Andersson, O. *Eur. Polym. J.* **2008**, *44*, 2865–2873.
(19) Bellander, M.; Stenberg, B.; Persson, S. *Polym. Eng. Sci.* **1998**, *38*, 1254–1260.
(20) Gao, J.; Itkis, M. E.; Yu, A.; Bekyarova, E.; Zhao, B.; Haddon, R. C. *J. Am. Chem. Soc.* **2005**, *127*, 3847–3854.
(21) Hakansson, B.; Andersson, P.; Backstrom, G. *Rev. Sci. Instrum.* **1988**, *59*, 2269–2275.
(22) Gedde, U. W. *Polymer Physics*; Kluwer Academic Publishers: Dordrecht, 2001.
(23) Campoy, I.; Gómez, M. A.; Marco, C. *Polymer* **1998**, *39*, 6279–6288.
(24) Illers, V. K.-H.; Haberkorn, H. *Makromol. Chem.* **1971**, *142*, 31–67.
(25) Masakazu, I. *J. Polym. Sci., Part A* **1963**, *1*, 2697–2709.
(26) Lin, Y.; Zhong, W.; Shen, L.; Xu, P.; Du, Q. *J. Macromol. Sci., Part B: Phys.* **2005**, *44*, 161–175.
(27) Isasi, J. R.; Mandelkern, L.; Galante, M. J.; Alamo, R. G. *J. Polym. Sci., Part B: Polym. Phys.* **1999**, *37*, 323–334.
(28) Lewis, E. L. V.; Ward, I. M. *J. Macromol. Sci., Part B: Phys.* **1980**, *18*, 1–46.
(29) Lin, L.; Argon, A. S. *Macromolecules* **1992**, *25*, 4011–4024.
(30) Schaefgen, J. R.; Flory, P. J. *J. Am. Chem. Soc.* **1948**, *70*, 2709–2718.
(31) Mattiussi, A.; Gechele, G. B.; Francesconi, R. *J. Polym. Sci., Part A-2: Polym. Phys.* **1969**, *7*, 411–422.
(32) Pramanik, N. K.; Haldar, R. S.; Bhardwaj, Y. K.; Sabharwal, S.; Niyogi, U. K.; Khandal, R. K. *Radiat. Phys. Chem.* **2009**, *78*, 199–205.
(33) Sengupta, R.; Sabharwal, S.; Tikku, V. K.; Somani, A. K.; Chaki, T. K.; Bhowmick, A. K. *J. Appl. Polym. Sci.* **2006**, *99*, 1633–1644.
(34) Van Krevelen, D. W. *Properties of Polymers*; Elsevier Publishing Co.: Amsterdam, 1972.
(35) Andersson, S. P.; Andersson, O. *Macromolecules* **1998**, *31*, 2999–3006.
(36) Chen, H.; Cebe, P. *J. Therm. Anal. Calorim.* **2007**, *89*, 417–425.
(37) Aharoni, S. M. *n-Nylons: Their Synthesis, Structure, and Properties*; John Wiley & Sons, Ltd.: Chichester, 1997.
(38) Andersson, O. *Int. J. Thermophys.* **1997**, *18*, 195–208.
(39) Murthy, N. S.; Curran, S. A.; Aharoni, S. M.; Minor, H. *Macromolecules* **1991**, *24*, 3215–3220.
(40) Levchik, S. V.; Weil, E. D.; Lewin, M. *Polym. Int.* **1999**, *48*, 532–557.
(41) Ostwald, W. *Z. Phys. Chem., Stoechiom. Verwandtschaftsl.* **1900**, *34*, 495.
(42) Freundlich, H. *Kolloidchemie*; Akademischer Verlagsgeselschaft: Leipzig, 1909.
(43) Basset, D. C. *Characterization and Analysis of Polymers*; John Wiley & Sons, Inc.: Hoboken, NJ, 2008.
(44) Lu, L.; Alamo, R. G.; Mandelkern, L. *Macromolecules* **1994**, *27*, 6571–6576.
(45) Ma, J.; Simon, G. P.; Edward, G. H. *Macromolecules* **2007**, *41*, 409–420.
(46) Andersson, S. P. Thermophysical properties of amorphous polymers under high pressure. Ph.D. Thesis, Umea University, Umea, 1998.
(47) Hansen, D.; Ho, C. C. *J. Polym. Sci., Part A* **1965**, *3*, 659–670.